RSC Advances

This article can be cited before page numbers have been issued, to do this please use: Y. Wang, L. Dong, Z. Zheng, X. Li, R. Xiong, J. Hua and A. Hu, *RSC Adv.*, 2016, DOI: 10.1039/C5RA25938J.

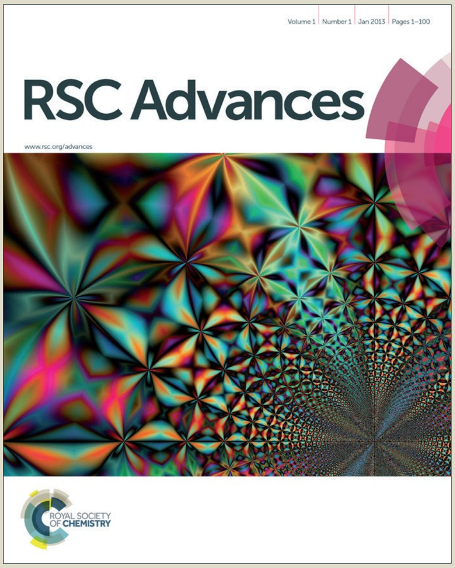

View Article Online
DOI: 10.1039/C5RA25938J

Journal Name

ARTICLE

Enediyne as π linker in D-π-A dyes for dye-sensitized solar cells†

Youfu Wang,[a] Luhua Dong,[a] Zhiwei Zheng,[b] Xing Li,[b] Rulin Xiong,[a] Jianli Hua*[b] and Aiguo Hu*[a]

Received 00th January 20xx,
Accepted 00th January 20xx

DOI: 10.1039/x0xx00000x

www.rsc.org/

Three Donor-π-Acceptor (D-π-A) type dyes, with triphenylamine (TPA) as electronic donor, enediyne (EDY) moiety as π linker and cyanoacrylic acid as both electronic acceptor and anchoring group, were designed and synthesized. These EDY-bridged dyes with different donor position and number are used as sensitizers in dye-sensitized solar cells (DSSCs) to study the influence of these factors on their performance. The results show that varying the donor position and number shifts the absorbance peak or enhances the absorption intensity, but does not broaden the absorption range. With two donors at both *meta*- and *para*-positions, the conjugation length in **EDY-3** is broadened, meanwhile, the twisty donors with asymmetric structure endow **EDY-3** retarded dye aggregation and charge recombination. Therefore, **EDY-3** shows the best performance in DSSCs among the three kinds of dyes with iodide/triiodide solution as electrolyte (J_{SC} = 12.28 mA•cm^{-2}, V_{OC} = 730 mV, FF = 60.43% and PCE = 5.41%).

Introduction

Dye-sensitized solar cells (DSSCs) have got significant attentions during the last two decades owing to their low-cost fabrication and high power conversion efficiency (PCE) from solar energy to electricity.[1-3] The performance of DSSC depends upon its constituent parts, such as the nature of sensitizer(s), photoanode, counter electrode, and electrolyte and their combination.[4] Among them, the nature of sensitizer(s) is pivotal to influence the DSSCs performance. The dyes should possess broad absorption spectra and high molar extinction coefficients to absorb more than enough photons from sunlight for efficient energy conversion. At present, state-of-the-art DSSCs based on ruthenium-containing complexes as the active material have an overall PCE approaching 11.9% under standard (Global Air Mass 1.5) illumination.[5-7] At the same time, more and more efforts have been devoted to find ruthenium-free sensitizers, as ruthenium is a noble and expensive metal.[3] Metal-free organic sensitizers have a number of advantages, such as high molar extinction coefficient, infinite flexibility of molecular tailoring, tunable spectral properties, relatively high efficiency, low cost and elimination of environmental issues.[8] Generally, donor-π-acceptor (D-π-A) type sensitizers are the most interesting and promising dyes for DSSCs, due to their efficient intramolecular charge transfer (ICT) properties.[9, 10]

Many efforts have been dedicated on the “molecular structure-device efficiency relationship” in every aspect of D-π-A structural dyes in DSSCs.[11, 12] The effect of donor moiety,[13] π-linker type,[14, 15] acceptor group, and anchoring group[16] on the performance of DSSCs have been exploited.[11, 12, 17] Furthermore, the donor size,[18] the donor-position,[19] the π-linker length,[20] the extra Donor/acceptor group for D-D-π-A[21] or D-A-π-A structure,[22] the branched alkane[23] and the anchoring group[24, 25] are also well-studied. Increasing the donor size via adding phenyl or electron-donating group has little influence on the photoresponse range but increase the absorption intensity,[18] while increasing the π-linker length promotes a bathochromic shift of the absorbance band as well a decrease in the IPCE due to the dye-aggregation and photoisomerization.[26] The donor in *para*-position is better than in *meta*-position related to the acceptor in similar structured dyes.[19] The introduction of branched alkane or co-adsorbent retards the dye aggregation.[27] Previous work showed that the donor position and number are important for D-π-A type dyes.[9, 28] However, prototypical D-π-A dyes with enediyne as π-linker and different donor position and number were first synthesized and their performance in DSSCs has also been systematically investigated.

Enediyne (EDY) molecules,[29] as the active parts in many natural antibiotics, form diradicals to cleavage DNA or form polyarylenes when they undergo Bergman cyclization.[30-32] EDY structure and related Bergman cyclization have been appreciated in a broad of fields, such as cancer therapy,[33] polymer chemistry[34-36] and material science.[32, 37-39] Herein, three EDY-bridged D-π-A dyes with TPA as electronic donor, EDY moiety as π linker and cyanoacrylic acid as both electronic acceptor and anchoring group are designed and synthesized. The results show that the donor position and number show strong influence on their performance in DSSCs for D-π-A type all-organic dyes.

---

[a] *Shanghai Key Laboratory of Advanced Polymeric Materials, School of Materials Science and Engineering, East China University of Science and Technology, Shanghai, 200237, China. E-mail: hagmhsn@ecust.edu.cn*

[b] *Key Laboratory for Advanced Materials and Institute of Fine Chemicals, East China University of Science and Technology, Shanghai 200237, China. E-mail: jlhua@ecust.edu.cn*

†Electronic Supplementary Information (ESI) available: [details of the synthesis and NMR spectra of related compounds are available]. See DOI: 10.1039/x0xx00000x

View Article Online
DOI: 10.1039/C5RA25938J

Experimental

Materials

Triethylamine (TEA) and acetonitrile were distilled over calcium hydride. Tetrahydrofuran (THF) was pre-dried over calcium hydride, refluxed with sodium wire and benzophenone till the solution turned to deep blue and then distilled before use. Other chemicals were commercially available and used as received.

Synthesis of EDY-bridged dyes

The synthesis of three EDY-bridged D-π-A dyes with different donor numbers and donor positions is illustrated in Scheme 1. N,N-diphenyl-4-((trimethylsilyl)ethynyl)aniline (**1**) and 4-ethynyl-N,N-diphenylaniline (**2**) were synthesized following the literature procedures.[40] As all the EDY-bridged dyes are synthesized in a similar way, only the synthesis of **EDY-2** is detailed here as an example. The synthetic processes of **EDY-1** and **EDY-3** and related structural characterizations are available in electronic supplementary information (ESI).

4-bromo-3-iodobenzaldehyde (3).[41] Potassium iodate (1.28 g, 6 mmol) and potassium iodide (2.99 g, 18 mmol) were added slowly to concentrated sulphuric acid (30 mL) with vigorous stirring at 0 °C in dark. After stirring for 0.5 h, the above solution was added to 4-bromobenzaldehyde (3.7 g, 20 mmol) in concentrated sulphuric acid (50 mL) and stirred strongly for another 1 h. The reaction mixture was diluted with ice water and neutralized with sodium bicarbonate, the aqueous solution was extracted with ethyl acetate (EtOAc) and the combined organic phase was further washed with saturated sodium sulphite solution. After drying and recrystallizing in THF/petroleum ether (PE), white needle-like crystal **3** (4.32 g, 70% yield) was obtained. ^{1}H-NMR ($CDCl_3$, 400 MHz, ppm): 9.90 (s, 1H); 8.32 (d, J = 1.8 Hz, 1H); 7.80 (d, J = 8.2 Hz, 1H); 7.70 (dd, J = 8.2, 1.9 Hz, 1H). ^{13}C-NMR ($CDCl_3$, 100 MHz, ppm): 189.82; 141.40; 137.15; 136.22; 133.56; 129.84; 102.15. HR-MS (ESI): m/z calcd. For C_7H_4BrIO $(M)^+$: 309.8490, found: 309.8491.

4-bromo-3-((trimethylsily)ethynyl)benzaldhyde (6). Compound **3** (1.55 g, 5 mmol), CuI (57.1 mg, 0.3 mmol), $Pd(PPh_3)_2Cl_2$ (105.3 mg, 0.15 mmol) and dry TEA (30 mL) were mixed in a 100 mL Schlenk flask. Then trimethylsilylacetylene (TMSA, 3.6 mL, 25 mmol) was added followed by free-pump-thaw degassing of the mixture. After reacting at 30 °C for 5 h, the dark brown solution was concentrated under reduced pressure and extracted with saturated sodium chloride (NaCl) solution and dichloromethane (DCM). The combined organic layer was dried over anhydrous $MgSO_4$. After filtration and removal of the solvent under vacuum, the crude product was purified through column chromatography (200-300 mesh silica, PE : EtOAc = 15 : 1) to yield a white power **6** (1.01 g, 72% yield). ^{1}H-NMR ($CDCl_3$, 400 MHz, ppm): 9.94 (s, 1H); 7.96 (d, J = 1.9 Hz, 1H); 7.75 (d, J = 8.3 Hz, 1H); 7.65 (dd, J = 8.3, 1.9 Hz, 1H); 0.29 (s, 9H). ^{13}C-NMR ($CDCl_3$, 100 MHz, ppm): 190.58; 135.19; 134.95; 133.45; 132.75; 129.37; 126.64; 101.95; 101.72; -0.14. HR-MS (ESI): m/z calcd. for $C_{12}H_{13}BrOSi$ $(M)^+$: 279.9919, found: 279.9900.

4-((4-(diphenylamino)phenyl)ethynyl)-3-((trimethylsilyl)ethynyl)benzaldhyde (7a). Compound **6** (560 mg, 2 mmol), $Pd(PPh_3)_2Cl_2$ (42.1 mg, 0.06 mmol), CuI (22.9 mg, 0.12 mmol) and dry TEA (15 mL) were mixed in a 50 mL Schlenk flask. Under nitrogen bubbling, compound **2** (595 mg, 2.2 mmol) dissolved in dry THF (15 mL) was added and then reacted at 90 °C for 12 hours. After cooling to room temperature, the resulting solution was concentrated under reduced pressure and extracted with saturated NaCl solution and DCM. The combined organic layer was dried over anhydrous $MgSO_4$. After filtration and removal of the solvent under vacuum, the crude product was purified through column chromatography (200-300 mesh silica, PE : DCM = 3 : 1) to yield orange-yellow power **7a** (530 mg, yield 56%). ^{1}H-NMR (DMSO-D_6, 400 MHz, ppm): 9.98 (s, 1H); 8.04 (s, 1H); 7.87 (d, J = 7.9 Hz, 1H); 7.73 (d, J = 8.0 Hz, 1H); 7.42 (d, J = 7.9 Hz, 2H); 7.37 (t, J = 7.3 Hz, 4H); 7.17-7.10 (m, 6H); 6.91 (d, J = 8.0 Hz, 2H); 0.24 (s, 9H). ^{13}C-NMR (DMSO-D_6, 100 MHz, ppm): 191.83; 148.53; 146.15; 134.99; 133.74; 132.86; 132.09; 130.63; 129.84; 128.42; 125.41; 124.83; 124.47; 120.45; 113.33; 102.30; 99.96; 97.87; 87.00; -0.23. HR-MS (ESI): m/z calcd. for $C_{32}H_{28}NOSi$ $(M+H)^+$: 470.1862, found: 470.1937.

4-((4-(diphenylamino)phenyl)ethynyl)-3-ethynylbenzaldhyde (7b). Compound **7a** (470 mg, 1 mmol), *p*-toluenesulfonic acid (PTSA, 172 mg, 1 mmol) and dry THF (10 mL) were mixed in 50 mL Schlenk flask under nitrogen at 0 °C. Tetrabutylammonium fluoride (TBAF•$3H_2O$, 0.63 g, 2 mmol) dissolved in dry THF (10 mL) was added dropwise. After reacting at 0 °C for 0.5 h, the resulting solution was concentrated under reduced pressure and extracted with 1 M hydrochloric acid solution and EtOAc. The organic layer was dried over anhydrous $MgSO_4$. After filtration and removal of the solvent under vacuum, the crude product was purified through column chromatography (200-300 mesh silica, PE : DCM = 3 : 1) to yield orange-yellow power 7b (360 mg, yield 92%). ^{1}H-NMR (DMSO-D_6, 400 MHz, ppm): 9.99 (s, 1H); 8.06 (s, 1H); 7.90 (d, J = 8.1 Hz, 1H); 7.75 (d, J = 8.0 Hz, 1H); 7.53-7.42 (m, 2H); 7.37 (dd, J = 7.4, 7.5 Hz, 4H); 7.18-7.07 (m, 6H); 6.97-6.86 (m, 2H); 4.64 (s, 1H). ^{13}C-NMR (DMSO-D_6, 100 MHz, ppm): 191.78; 148.51; 146.17; 135.02; 133.61; 132.96; 132.05; 130.86; 129.82; 128.75; 125.34; 124.55; 124.41; 120.62; 113.38; 97.81; 86.90; 86.04; 80.98. HR-MS (ESI): m/z calcd. for $C_{29}H_{20}NO$ $(M+H)^+$: 398.1467, found: 398.1543.

2-cyano-3-(4-((4-(diphenylamino)phenyl)ethynyl)-3-ethynylphenyl)acrylic acid (EDY-2). To a solution of compound **7b** (100 mg, 0.25 mmol) in dry acetonitrile (30 mL), cyanoacetic acid (43 mg, 0.50 mmol) and morpholine (0.2 mL) were added under nitrogen and refluxed at 85 ºC for 8 h. After cooling to room temperature, the resulting solution was concentrated under reduced pressure and purified through column chromatography (200-300 mesh silica, DCM : MeOH = 10 : 1) to yield orange-yellow power **EDY-2** (68.9 mg, yield 58%). ^{1}H-NMR (DMSO-D_6, 400 MHz, ppm): 8.06 (s, 2H); 7.92 (d, J = 8.4 Hz, 1H); 7.66 (d, J = 8.2 Hz, 1H); 7.42 (d, J = 8.7 Hz, 2H);

7.35 (t, *J* = 7.9 Hz, 7.6 Hz, 4H); 7.13 (t, *J* = 7.4 Hz, 2H); 7.08 (d, *J* = 7.6 Hz, 4H); 6.90 (d, *J* = 8.7 Hz, 2H); 4.57 (s, 1H). ^{13}C-NMR (DMSO-D$_6$, 100 MHz, ppm): 163.86; 148.37; 146.85; 146.28; 133.04; 132.90; 132.60; 131.95; 129.87; 129.71; 127.67; 125.30; 124.53; 124.39; 120.85; 118.37; 113.81; 113.05; 96.58; 87.14; 85.65; 81.30. HR-MS (ESI): m/z calcd. for $C_{32}H_{20}N_2O_2$ (M)$^+$: 464.1525, found: 464.1618.

Characterization

^{1}H-NMR (400 MHz, ppm) and ^{13}C-NMR (100 MHz, ppm) spectra were recorded on an Ultra Shield 400 spectrometer (BRUKER BIOSPIN AG, Magnet System 400 MHz/54 mm) using tetramethylsilane as an internal standard. High resolution mass spectra (HR-MS) were obtained using a Waters LCT Premier XE spectrometer. Matrix assisted laser deionization/time of flight (MALDI-TOF) mass spectroscopy were performed on mass spectrometer 4800 plus MALDI-TOF/TOF MS Analyzer (AB Sciex, USA) equipped with a Nd: YAG laser emitting at 355 nm, operating at an accelerating voltage of 20 kV in reflection mode. 4000 series Explorer and DATA Explorer (AB Sciex, USA) were used for data acquisition and processing. The extraction delay time used was 450 ns. All mass spectra were collected by averaging the signals of 500 individual laser shots. Dried-droplet samples were prepared by spotting 1 µL aliquot of a mixture of 5 µL of matrix (dithranol, 10 mg/ml in THF) and 1 µL of sample (10 mg/ml in THF) on the target plate. The UV-vis absorption of EDY-bridged dyes in solution and on TiO$_2$ films were measured with a Varian Cary 500 spectrophotometer. Cyclic voltammograms (CV) were obtained on a Versastat II electrochemical workstation (Princeton Applied Research) using a three-electrode cell with a glassy carbon working electrode, a Pt wire auxiliary electrode, and a saturated calomel reference electrode (SCE) in saturated potassium chloride solution with a scan rate of 100 mV•s^{-1}. Ferrocene (Fc) was used as an internal reference and 0.1 M tetra-n-butylammonium hexafluorophosphate (TBAPF$_6$) was used as the supporting electrolyte in chloroform (CHCl$_3$).

DSSCs device fabrication and photovoltaic performance tests

A 17 µm thick double-layer TiO$_2$ photoelectrode, composing of a 12 µm-thick nanoporous layer and a 5 µm-thick scattering layer (area: 0.5 × 0.5 cm2), was prepared by screen printing on a conducting glass substrate, fluorine-doped tin oxide (FTO). The TiO$_2$ films were immersed in the dye solution (3 × 10^{-4} M in CHCl$_3$) for 16 h. Photovoltaic measurements were performed in a sandwich-type solar cell in conjunction with an electrolyte consisting of a solution of I$_2$ (0.05 M), LiI (0.1 M), dimethylpropylimidazolium iodide (0.6 M), and 4-tert-butyl pyridine (0.5 M) in acetonitrile. The dye-absorbed TiO$_2$ film and a piece of platinum-coated conducting glass were separated by a Surlyn spacer (40 µm thick) and sealed by heating the polymer frame. The photocurrent density-voltage (*J-V*) of the sealed solar cell device was measured with a black metal mask of 0.25 cm^2 by illuminating the cell through the conducting glass from the anode side with a solar simulator (WXS-155S-10) at AM 1.5 illumination (light intensities: 100 mW•cm^{-2}). Monochromatic IPCE was measured with a monochromatic incident light of 1 × 10^{16} photons per centimetre under 100 mW•cm^{-2} in the director current mode measurements, which were made on a CEP-2000 system (Bunkoh-Keiki Co. Ltd.).

View Article Online
DOI: 10.1039/C5RA25938J

Electrochemical impedance spectroscopy (EIS) experiments were carried out in the dark using a ZAHNER ZENNIUM electrochemical workstation with frequency ranging from 50 mHz to 100 kHz and a potential amplitude of 5 mV. The obtained impedance spectra were fitted with the ZSimpWin software (v3.10) in terms of appropriate equivalent circuits.

Results and discussion

EDY-bridged dyes were synthesized according to the protocol shown in Scheme 1. Sonogashira coupling between aryl halide and alkyne and subsequent Knoevenagel condensation between arylaldehyde and cyanoacetic acid were frequently used in this protocols. The detail of synthetic processes of **EDY-1** and **EDY-3** and related structural characterizations are shown in ESI. Generally, these reactions produce the desired products in a facial and high-yielding manner.

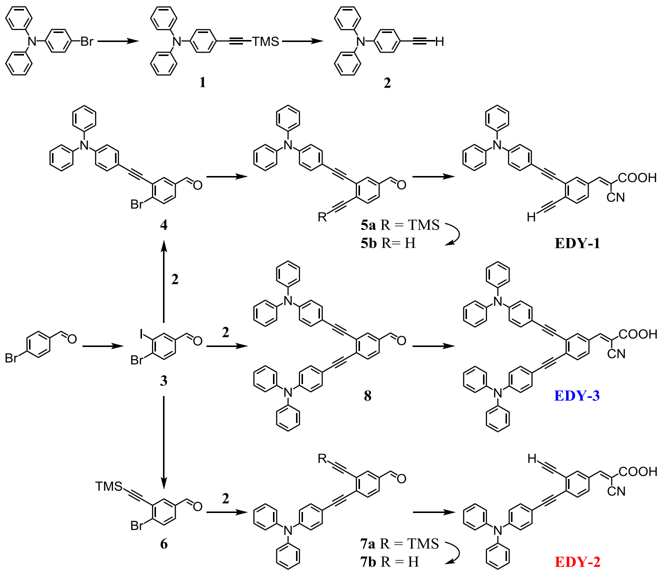

Scheme 1 The synthetic protocol of enediyne-bridged donor-π-acceptor dyes with different donor numbers and positions.

Three EDY-bridged dyes with different donor position and number were synthesized. **EDY-1** has one donor at *meta*-position related to acceptor, while the donor in **EDY-2** is at the *para*-position, **EDY-3** has two donors at both *meta-* and *para*-position. It is hope to find out if the donor position and number in EDY-bridged dyes effects on their performance in DSSCs.

UV-vis spectra of EDY-bridged dyes and **N719** in chloroform and on the surface of TiO$_2$ film are shown in Fig. 1. There are two obvious absorbance peaks for EDY-bridged dyes in chloroform. The lower energy bands at 350–500 nm with variable intensities are assign to intramolecular charge transfer

DOI: 10.1039/C5RA25938J

(ICT) transitions from the triphenylamine donors to the cyanoacrylic acid acceptors. Comparing these dyes with the same units but different donor position or number, the absorption bands of *para*-conjugated dyes (**EDY-2**) were more red-shifted when compared with the corresponding *meta*-conjugated dyes (**EDY-1**), as a result of better resonance in the former. The onset absorbance of these EDY-bridged dyes are around 550 nm and the **EDY-2** and **EDY-3** show almost the same absorbance peaks with different intensity. This indicates that the donor position affects significantly on their photophysical properties, while the number of electron-donor does not lead to significant changes in the position of the energy absorbance bands but has a strong influence on the related absorption intensity.[18] For **EDY-2** and **EDY-3**, the lowest energy absorbance peak is around 418–425 nm, stronger than corresponding absorption of **N719**. The absorbance band positions and their relative molar extinction coefficients are tabulated in Table 1. The broadened absorption spectra of these dyes adsorbed on the surface of TiO_2 film compared to the absorption spectra in solution might be ascribed to the slight aggregation of the dyes.

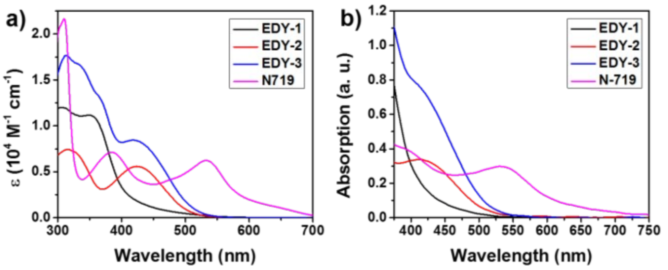

Fig. 1 UV-vis spectra of EDY-bridged dyes and **N719** in solution (chloroform, 50 μM) (a) and on the surface of TiO2 film (b).

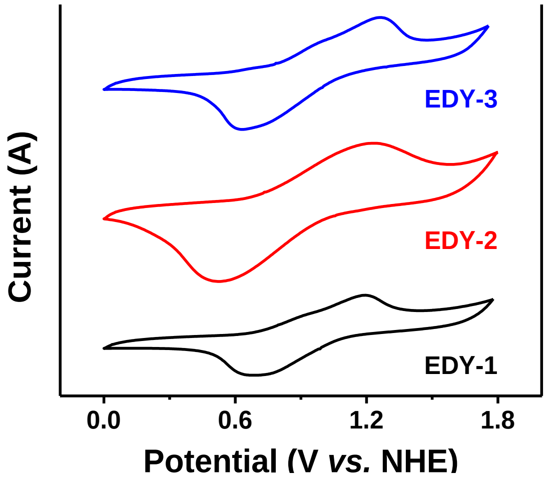

Fig. 2 Cyclic voltammetry curves of EDY-bridged dyes.

The cyclic voltammetry curves (CV) of EYD-bridged dyes are shown in Fig. 2, and the related redox potential values are presented in Table 1. The redox potentials of the **EDY-1**, **EDY-2** and **EDY-3** are 0.80, 0.74, and 0.81 V vs NHE, respectively, which are higher than that of the iodide/triiodide (0.40 V vs NHE) redox electrolyte energy level, guaranteeing ample driving force for the dye regeneration.

Table 1 Photophysical and electrochemical properties of EDY-bridged dyes.

EDY	λ_{max}[a] (nm)	ε[a] ($M^{-1}cm^{-1}$)	HOMO[b] (V/vs. NHE)	E_{0-0}[c] (eV)	LUMO[c] (V/vs. NHE)
EDY-1	350	11150	0.80	3.05	-2.25
EDY-2	424	5590	0.74	2.52	-1.78
EDY-3	418	8450	0.81	2.48	-1.67

[a] Absorbance peaks (λ_{max}) and molar extinction coefficients (ε) in $CHCl_3$. [b] HOMO was measured in $CHCl_3$ and calibrated with ferrocene with cyclic voltammetry (CV) at a scan rate of 100 mV•s^{-1}. [c] E_{0-0} was estimated from the absorbance thresholds (the intersection of normalized absorption/emission spectra) in the absorption spectra of dyes adsorbed on TiO_2 film. LUMO was estimated by subtracting E_{0-0} from the HOMO.

The structural differences in the donor part of EDY-bridged dyes have little influence on their redox potentials. By changing the donor position, **EDY-2** shows the increased HOMO level by 60 mV compared to **EDY-1**, which may due to the (quasi)planar geometry of **EDY-2** promoted by the phenyl-contained π linker. Estimated from the absorbance thresholds from absorption spectra of absorbed dyes on TiO_2 film, the bandgap energies (E_{0-0}) were determined to be 3.05, 2.52, and 2.48 V, respectively. The excited-state reduction potentials of EDY-bridged dyes were obtained by combining the redox potentials with the energy of the transition (E_{0-0}). The calculated LUMO level of these dyes (−2.25, −1.78, and −1.67 V, respectively) are placed sufficiently above the TiO_2 conduction band edge to ensure no energetic barriers for the electron injection.

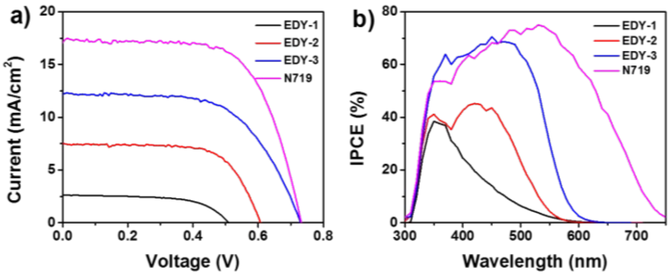

Fig. 3 The photovoltaic performance of DSSCs sensitized with EDY-bridged dyes and **N719** under AM 1.5G irradiation (100 mW•cm^{-2}). (a) *J-V* curves and (b) IPCE plots.

The photovoltaic performance of DSSC devices sensitized by EDY-bridged dyes and **N719** was investigated using double-layer TiO_2 films as photo-anodes (12 μm transparent TiO_2 layer and 5 μm TiO_2 scattering layer) in combination with iodide/triiodide system as electrolyte and platinum (Pt) coated FTO as a counter electrode (CE), and the photovoltaic parameters are presented in Table 2. The photocurrent–voltage curve as well the incident photon to current conversion efficiency (IPCE) value of the dye-containing DSSC devices are shown in Fig. 3. The short-circuit photocurrent density (J_{SC}) increases significantly with the order of **EDY-1** < **EDY-2** < **EDY-3**, which may due to the red-shift absorbance and the increased absorption intensity (Fig. 1 and Fig. 3a). The open-circuit photovoltage (V_{OC}) are increasing in the same order may due to the retarded dye aggregation and reduced charge recombination. The donor position and number will influence their configuration on TiO_2 film and will be discussed later. It is interesting to note that the V_{OC} of **EDY-3** (730 mV) are competitive with **N719** (731 mV), which may due to the two twisty donors reduce the tendency of dye aggregation and charge recombination between iodide-based electrolyte and injected electron in the conductive band of TiO_2.[28]

IPCE curves (Fig. 3b) of EDY-bridged dyes and **N719** indicate that the EDY-bridged dyes have similar photoresponse range (300-600 nm), which consists with their photophysical properties as shown in Fig. 1. **EDY-2** has a similar curve with **EDY-1** in ultraviolet region except an extra broad peak in range of 380-600 nm. IPCE values of **EDY-3** reach a higher value than **N719** during the range of 350-460 nm, whereas a maximum of 70% is reached at 450 nm. These results consist with the stronger absorption at related range shown in Fig. 1.

Table 2 Photovoltaic parameters of DSSCs devices absorbed with EDY-bridged dyes and **N719** measured under simulated AM1.5G solar light (100 mW•cm^{-2}).

EDY	J_{SC} (mA•cm^{-2})	V_{OC} (mV)	FF (%)	PCE (%)
EDY-1	2.63	509	60.87	0.82
EDY-2	7.46	607	69.10	3.26
EDY-3	12.28	730	60.43	5.41
N719	17.33	731	65.80	8.34

EDY-2 shows better performance than **EDY-1** may due to the intrinsic better resonance degree for effective ICT transition when donor moiety is presented on *para*-position instead of *meta*-position as discussed on their photophysical properties. Moreover, when EDY-bridged dyes are absorbed on the surface of TiO_2, **EDY-1** prefers to lie on its side and then its excited state will recombine with injected electron on E_{CB} of TiO_2.[25, 42] And the collapsed **EDY-1** reduces the absorbed amount of dyes on TiO_2. While the **EDY-2** prefers to vertically orientate to the surface of TiO_2, which results in more absorbed dyes and a higher electron injection yield. Both the symmetric structure and the phenyl-contained π linker of **EDY-2** promote the (quasi)planar geometry for efficient electron transfer, however, the (quasi)planar geometry will induce dye aggregation, which limit its performance. **EDY-3** with two donors broadens the conjugation length, meanwhile, the asymmetric structure and twisty donors retard the dye aggregation and the charge recombination between electrolyte and injected electrons. Altogether, due to the enhanced conjugation degree and structure-induced retarded charge recombination, the photovoltaic performance of EDY-bridged dyes are presented as order **EDY-1** < **EDY-2** < **EDY-3**.

The photovoltaic performance of **EDY-2** bridged with enediyne is better than reported dyes with almost the same structure, such as phenylethylene-bridged dye (J_{SC} = 8.56 mA•cm^{-2}, V_{OC} = 710 mV, FF = 0.47, PCE = 2.89%)[14] and phenylethylene-bridged dye with dimethoxy substituted triphenylamine (J_{SC} = 6.95 mA•cm^{-2}, V_{OC} = 623 mV, FF = 0.742, PCE = 3.21%),[43] which means the enediyne moiety works well for effectively expanding the conjugation length. The **EDY-3** with two donors shows nearly two times efficiency of phenylethylene-bridge dye, indicating that the multi-donor has significantly effect in photovoltaic performance. It is more effective to further improve the performance of DSSCs by constructing molecular dyes or polymeric dyes with multipled donors than the tandem donor in D-D-π-A structured dyes.

View Article Online
DOI: 10.1039/C5RA25938J

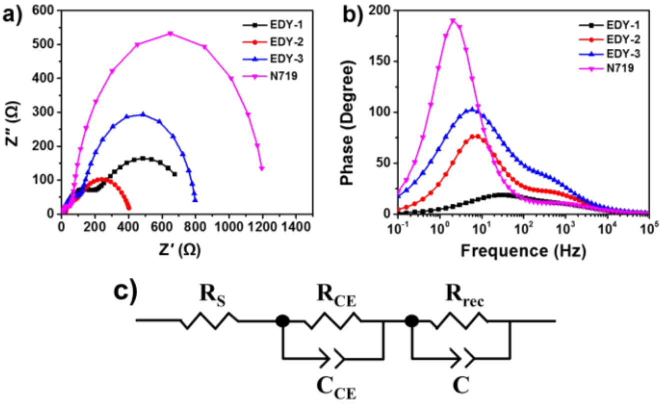

Fig. 4 Electrochemical impedance spectroscopy (EIS) spectra for DSSCs absorbed on EDY-bridged dyes and **N719**. (a) Nyquist plots; (b) Bode phase plots; (c) Equivalent circuits. The lines of parts (a and b) show theoretical fits using the equivalent circuits in (c).

The Nyquist plot, Bode plot, and equivalent circuit are shown in Fig. 4. Each of the Nyquist plots in Fig. 4a contains two semicircles. The left semicircle at the higher frequency region assigns to the resistance at the interface between the electrolyte and counter electrode (R_{CE}) and the right semicircle in the lower frequency region is attributed to the charge transfer resistance at the dye/TiO_2/electrolyte interface resistance (R_{rec}). R_{rec} is related to charge recombination process from the CB of TiO_2 to the oxidized ions in the electrolyte solution.[44, 45] The R_{rec} value is estimated by the real component radius of the fitted right semicircle. These estimated and calculated EIS parameters have been listed in Table 3. In the equivalent circuit for EIS, C is attributed to the dye/TiO_2/electrolyte interface. Generally, the V_{OC} performance is closely sensitive to charge transport processes at the TiO_2/dye/electrolyte interface.[46, 47] Obviously, with the same electrode material and the same electrolyte, four DSSCs show close R_S (the TCO sheet resistance) and R_{CE} value (shown in Table 3), especially for **EDY-2**, **EDY-3** and **N719**. The strategy to restrain charge recombination increases the radius of the second semicircle (in Nyquist plots), moving the phase angle peak (in Bode plots) to low frequency and increasing the R_{rec} value. Apparently, in Fig. 4a and 4b, the smaller width of the second semicircle of EDY-bridged dyes and the higher frequency of the phase angle peak indicate a smaller charge-transfer resistance (compared to the **N719** cell) at the TiO_2/dye/electrolyte interface. **EDY-3** has a larger value of R_{rec} than **EDY-1** and **EDY-2**, showing the two twisted donors will effectively retard the charge recombination and dye aggregation. The electron lifetime can be calculated from the equation $1/2\pi f_p$,[48] where f_p is the peak frequency of lower

View Article Online
DOI: 10.1039/C5RA25938J

frequency region in the Bode phase plots. The calculated electron lifetime decreased in the order of **N719** (63.6 ms) > **EDY-3** (27.0 ms) > **EDY-2** (22.7 ms) > **EDY-1** (4.7 ms), well consist with the tendency of VOC together with R_{rec}.

Table 3 Parameters obtained by fitting the impedance spectra of the DSSCs with sensitizers using the equivalent circuit (Fig. 4c).

EDY	R_S (Ω)	R_{CE} (Ω)	R_{rec} (Ω)	τ_e (ms)
EDY-1	**17.6**	**177.5**	**529.1**	**4.7**
EDY-2	**16.5**	**50.5**	**259.5**	**22.7**
EDY-3	**17.4**	**75.7**	**794.1**	**27.0**
N719	**17.1**	**57.1**	**1114.7**	**63.6**

Conclusions

In summary, three enediyne bridged donor-π-acceptor dyes with different donor position and number are designed and synthesized. Their photophysical and electrochemical properties show that donor position and number do not broaden the photoresponse spectra but shift the absorbance peak or enhance the absorption intensity. Their photophysical and electrochemical properties are suitable for applying in DSSCs. Their photovoltaic performance of these dyes in DSSCs show that **EDY-1** with one donor at *meta*-position may lie on TiO_2 surface which will cause charge recombination and inhibit the adsorption of the dye molecules, while **EDY-2** with one donor at *para*-position may vertically orientate to the surface of TiO_2 and results in a good electron injection yield and high density adsorption of the dye molecules. However, dye-aggregation is significant in this kind of dye due to its (quasi)planar geometry. **EDY-3** with two donors at both *meta*- and *para*-position broadens the conjugation length, meanwhile the asymmetric structure and twisty donors helps to retard the dye aggregation and charge recombination between electrolyte and injected electrons. The results showed that by introducing conjugated groups in the *para*-position relative to acceptor, the conjugation degree is enhanced. Moreover, by introducing an extra donor group at *meta*-position, the dye aggregation can be effectively retarded to further help to improve the performance of Donor-π-Acceptor type organic dyes in DSSCs. The enediyne bridged dyes are a promise type of dyes for improving the performance of DSSCs.

Acknowledgements

The authors gratefully acknowledge the financial support from the National Natural Science Foundation of China (91023008, 21474027, 21172073, 91233207), the Key Laboratory of Advanced Polymer Materials of Shanghai (WD10140502) and the Shanghai Leading Academic Discipline Project (B502). A. H. thanks the “Eastern Scholar Professorship” support from Shanghai local government.

Notes and references

1. B. O'Regan and M. Gratzel, *Nature*, 1991, **353**, 737-740.
2. B. E. Hardin, H. J. Snaith and M. D. McGehee, *Nature Photonics*, 2012, **6**, 162-169.
3. S. Mathew, A. Yella, P. Gao, R. Humphry-Baker, B. F. E. Curchod, N. Ashari-Astani, I. Tavernelli, U. Rothlisberger, M. K. Nazeeruddin and M. Gratzel, *Nature Chem.*, 2014, **6**, 242-247.
4. A. Hagfeldt, G. Boschloo, L. Sun, L. Kloo and H. Pettersson, *Chem. Rev.*, 2010, **110**, 6595-6663.
5. C.-Y. Chen, M. Wang, J.-Y. Li, N. Pootrakulchote, L. Alibabaei, C.-h. Ngoc-le, J.-D. Decoppet, J.-H. Tsai, C. Grätzel and C.-G. Wu, *ACS nano*, 2009, **3**, 3103-3109.
6. F. Gao, Y. Wang, D. Shi, J. Zhang, M. Wang, X. Jing, R. Humphry-Baker, P. Wang, S. M. Zakeeruddin and M. Grätzel, *J. Am. Chem. Soc.*, 2008, **130**, 10720-10728.
7. Q. Yu, Y. Wang, Z. Yi, N. Zu, J. Zhang, M. Zhang and P. Wang, *ACS nano*, 2010, **4**, 6032-6038.
8. A. Mishra, M. K. Fischer and P. Bäuerle, *Angew. Chem. Int. Ed.*, 2009, **48**, 2474-2499.
9. Y. Hong, J.-Y. Liao, D. Cao, X. Zang, D.-B. Kuang, L. Wang, H. Meier and C.-Y. Su, *J. Org. Chem.*, 2011, **76**, 8015-8021.
10. S. Haid, M. Marszalek, A. Mishra, M. Wielopolski, J. Teuscher, J. E. Moser, R. Humphry - Baker, S. M. Zakeeruddin, M. Grätzel and P. Bäuerle, *Adv. Funct. Mater.*, 2012, **22**, 1291-1302.
11. J. N. Clifford, E. Martínez-Ferrero, A. Viterisi and E. Palomares, *Chem. Soc. Rev.*, 2011, **40**, 1635-1646.
12. B. G. Kim, K. Chung and J. Kim, *Chem.-Eur. J.*, 2013, **19**, 5220-5230.
13. M. Liang and J. Chen, *Chem. Soc. Rev.*, 2013, **42**, 3453-3488.
14. J. Song, F. Zhang, C. Li, W. Liu, B. Li, Y. Huang and Z. Bo, *J. Phys. Chem. C*, 2009, **113**, 13391-13397.
15. C. Teng, X. Yang, C. Yang, H. Tian, S. Li, X. Wang, A. Hagfeldt and L. Sun, *J. Phys. Chem. C*, 2010, **114**, 11305-11313.
16. P. Ganesan, A. Yella, T. W. Holcombe, P. Gao, R. Rajalingam, S. A. Al-Muhtaseb, M. Graetzel and M. K. Nazeeruddin, *Acs Sustain Chem Eng*, 2015, **3**, 2389-2396.
17. S. Zhang, X. Yang, Y. Numata and L. Han, *Energy Environ. Sci.*, 2013, **6**, 1443-1464.
18. J. Yang, P. Ganesan, J. l. Teuscher, T. Moehl, Y. J. Kim, C. Yi, P. Comte, K. Pei, T. W. Holcombe and M. K. Nazeeruddin, *J. Am. Chem. Soc.*, 2014, **136**, 5722-5730.
19. Y. D. Lin, C. T. Chien, S. Y. Lin, H. H. Chang, C. Y. Liu and T. J. Chow, *J. Photochem. Photobiol. A-Chem.*, 2011, **222**, 192-202.
20. D. P. Hagberg, T. Marinado, K. M. Karlsson, K. Nonomura, P. Qin, G. Boschloo, T. Brinck, A. Hagfeldt and L. Sun, *J. Org. Chem.*, 2007, **72**, 9550-9556.
21. P. P. Dai, L. Yang, M. Liang, H. H. Dong, P. Wang, C. Y. Zhang, Z. Sun and S. Xue, *Acs Appl. Mater. Inter.*, 2015, **7**, 22436-22447.
22. Y. Wu and W. Zhu, *Chem. Soc. Rev.*, 2013, **42**, 2039-2058.
23. Q. Chai, W. Li, Y. Wu, K. Pei, J. Liu, Z. Geng, H. Tian and W. Zhu, *Acs Appl. Mater. Inter.*, 2014, **6**, 14621-14630.
24. H. N. Tian, X. C. Yang, R. K. Chen, Y. Z. Pan, L. Li, A. Hagfeldt and L. C. Sun, *Chem. Commun.*, 2007, 3741-3743.
25. J. Wiberg, T. Marinado, D. P. Hagberg, L. Sun, A. Hagfeldt and B. Albinsson, *J. Phys. Chem. C*, 2009, **113**, 3881-3886.
26. S. Kim, H. Choi, D. Kim, K. Song, S. O. Kang and J. Ko, *Tetrahedron*, 2007, **63**, 9206-9212.

View Article Online
DOI: 10.1039/C5RA25938J

27. N. Koumura, Z.-S. Wang, S. Mori, M. Miyashita, E. Suzuki and K. Hara, *J. Am. Chem. Soc.*, 2006, **128**, 14256-14257.
28. J. Tang, J. Hua, W. Wu, J. Li, Z. Jin, Y. Long and H. Tian, *Energy Environ. Sci.*, 2010, **3**, 1736-1745.
29. E. Kraka and D. Cremer, *J. Am. Chem. Soc.*, 1994, **116**, 4929-4936.
30. N. Choy, B. Blanco, J. Wen, A. Krishan and K. C. Russell, *Org. Lett.*, 2000, **2**, 3761-3764.
31. A. Basak, S. Mandal and S. S. Bag, *Chem. Rev.*, 2003, **103**, 4077-4094.
32. S. Chen and A. Hu, *Science China Chemistry*, 2015, **58**, 1710-1723.
33. D. Song, S. Sun, Y. Tian, S. Huang, Y. Ding, Y. Yuan and A. Hu, *J. Mater. Chem. B*, 2015, **3**, 3195-3200.
34. X. Cheng, J. Ma, J. Zhi, X. Yang and A. Hu, *Macromolecules*, 2009, **43**, 909-913.
35. B. Zhu, J. Ma, Z. Li, J. Hou, X. Cheng, G. Qian, P. Liu and A. Hu, *J. Mater. Chem.*, 2011, **21**, 2679-2683.
36. Q. Sun, C. Zhang, Z. Li, H. Kong, Q. Tan, A. Hu and W. Xu, *J. Am. Chem. Soc.*, 2013, **135**, 8448-8451.
37. B. Zhu, S. Sun, Y. Wang, S. Deng, G. Qian, M. Wang and A. Hu, *J. Mater. Chem. C*, 2013, **1**, 580-586.
38. X. Yang, Z. Li, J. Zhi, J. Ma and A. Hu, *Langmuir*, 2010, **26**, 11244-11248.
39. L. Dong, Z. Zheng, Y. Wang, X. Li, J. Hua and A. Hu, *J. Mater. Chem. A*, 2015, **3**, 11607-11614.
40. D. H. Lee, M. J. Lee, H. M. Song, B. J. Song, K. D. Seo, M. Pastore, C. Anselmi, S. Fantacci, F. De Angelis and M. K. Nazeeruddin, *Dyes Pigments*, 2011, **91**, 192-198.
41. L. Kraszkiewicz, M. Sosnowski and L. Skulski, *Synthesis*, 2006, 1195-1199.
42. Z. J. Ning, Q. Zhang, W. J. Wu, H. C. Pei, B. Liu and H. Tian, *J. Org. Chem.*, 2008, **73**, 3791-3797.
43. J. L. Song, P. Amaladass, S. H. Wen, K. K. Pasunooti, A. Li, Y. L. Yu, X. Wang, W. Q. Deng and X. W. Liu, *New J. Chem.*, 2011, **35**, 127-136.
44. M. Adachi, M. Sakamoto, J. T. Jiu, Y. Ogata and S. Isoda, *J. Phys. Chem. B*, 2006, **110**, 13872-13880.
45. M. Afrooz and H. Dehghani, *RSC Adv.*, 2015, **5**, 50483-50493.
46. J. J. H. Pijpers, R. Ulbricht, S. Derossi, J. N. H. Reek and M. Bonn, *J. Phys. Chem. C*, 2011, **115**, 2578-2584.
47. K. L. Wu, C. H. Li, Y. Chi, J. N. Clifford, L. Cabau, E. Palomares, Y. M. Cheng, H. A. Pan and P. T. Chou, *J. Am. Chem. Soc.*, 2012, **134**, 7488-7496.
48. C. Li, C. Sun, S. Song, V. Choong, G. Maracas and X. Zhang, *Frontiers in Bioscience*, 2005, **10**, 180-186.

View Article Online
DOI: 10.1039/C5RA25938J

Table of Contents Graphic and Synopsis

Enediyne as π linker in D-π-A dyes for dye-sensitized solar cells

Youfu Wang,[a] Luhua Dong,[a] Zhiwei Zheng,[b] Xing Li,[b] Rulin Xiong,[a] Jianli Hua*[b] and Aiguo Hu*[a]

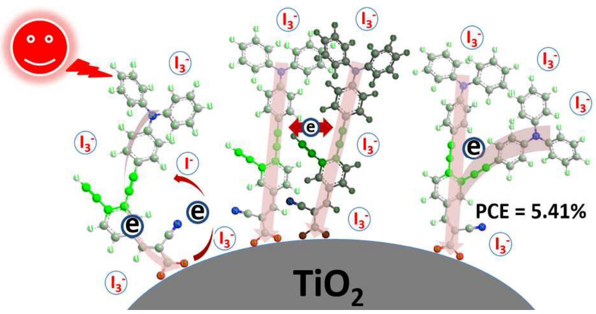

Three enediyne-bridged D-π-A dyes with different donor position and number are synthesized and their performance on DSSCs are investigated.